Phys. Status Solidi C **6**, No. 12, 2746–2749 (2009) / **DOI** 10.1002/pssc.200982540

physica status solidi c
www.pss-c.com
current topics in solid state physics

Optical and electrical properties of Nd-doped $BiFeO_3$ thin films and heterostructures

Bonifacas Vengalis*, Jelena Devenson, Antanas K. Oginskis, Vaclovas Lisauskas, Fiodoras Anisimovas, Renata Butkute, and Leonas Dapkus

Semiconductor Physics Institute, Gostauto 11, 01108 Vilnius, Lithuania

Received 15 June 2009, revised 28 September 2009, accepted 29 September 2009
Published online 29 October 2009

PACS 61.05.cp, 68.55.-a, 73.40.Lq, 77.84.Bw, 78.66.Li, 81.15.Cd

* Corresponding author: e-mail veng@pfi.lt, Phone: +370 5 261 78 64, Fax: +370 5 2627123

High quality $BiFeO_3$ (BFO) and $Bi_{0.9}Nd_{0.1}FeO_3$ (BNFO) thin films (d = 150-350 nm) were grown at 650-750°C by RF sputtering on dielectric ($SrTiO_3$; ZrO_2<Y>) and conducting (Nb-doped $SrTiO_3$(100); n-type Si) substrates. A direct band gap at 2.57 eV and 2.62 eV (at T=295 K) have been estimated for the BFO/YSZ and BNFO/YSZ films from optical transmittance spectra while an unset of weak absorption has been indicated for the films at 2.20 eV. Transverse electrical transport of the (BFO, BNFO)/(STON, Si) heterostructures revealed nonlinear current versus voltage behavior and clearly defined rectifying properties. Schottky junction model has been applied for the heterojunctions at T=300 K although complicated shape of I-U curves demonstrated increasing role of space charge limited current with T decreasing down to 78 K.

1 Introduction Ferroelectric ferromagnets with coupled electric, magnetic, and structural order parameters are known as multiferroics [1]. Electrical and magnetic properties of the materials may be controlled via applied electric and magnetic fields [2], and therefore they provide great potential for various applications in high density information storage, spintronics, and sensors.

Bismuth ferrite, $BiFeO_3$ (BFO) is one of the most extensively studied multiferroic materials. It is ferroelectric ($T_C \approx$ 1103 K), antiferromagnetic ($T_N \approx$ 643 K) and exhibits weak magnetism at room temperature due to a residual moment occurring from a canted spin structure [3]. Electrical leakage resulting from possible defects and non-stoichiometry remains as one of the main obstacles to practical applications of the material although it was found recently that electrical conductivity of BFO could be reduced by partial substitution of both Bi and Fe ions [4-7].

Thin films of both pure and Nd-doped $BiFeO_3$ were grown in this work. Partial substitution of Bi by Nd was undertaken to stabilize perovskite structure and to reduce electrical conductivity of the compound. Optical transmission was measured in a visible spectra range to determine band gap of both doped and undoped materials. Transverse electrical transport measurements were performed for the heterostructures formed by growing BFO and $Bi_{0.9}Nd_{0.1}FeO_3$ (BNFO) films on conductive (n-Si and $SrTiO_3$<Nb>) substrates to elucidate possible mechanisms of current flow.

2 Experimental The BFO and BNFO films with thickness d ranging from about 200 nm to 250 nm were grown *in-situ* at 650-700 °C under Ar/O_2 (1:1) gas pressure of 6-10 Pa by RF magnetron sputtering. Wafers of both dielectric $SrTiO_3$(100), ZrO_2<Y> (YSZ) and semiconducting Nb-doped 0.7 weight % $SrTiO_3$(100) (STON), n-type Si(111) as well as $SrTiO_3$ coated by highly conductive $SrRuO_3$ films were used as substrates. Disk-shaped ceramic targets of both undoped and Nd-doped BFO have been synthesized by applying a standard solid state reaction method using high purity powdered Bi_2O_3, Fe_2O_3 and Nd_2O_3 oxides. Bi content in the targets was slightly enhanced (by about 5%) to compensate possible loss of highly volatile Bi during film growth. Crystalline structure of the synthesized ceramic targets and the prepared thin films was investigated by measuring XRD spectra using CuKα radiation. AFM investigations were performed to study surface quality of the prepared films and heterostructures.

Optical transmission of the BFO and BNFO films deposited onto transparent (STO and YSZ) substrates was investigated at room temperature in the wavelength range 0.3-3.0 μm. The Ag/BFO(BNFO)/SRO/STO heterostructures were prepared to evaluate electrical resistivity of the multiferroic materials while the Ag/BFO(BNFO)/n-Si and BFO(BNFO)/STON heterostructures were used to investigate transverse current transport and formation of a Shottky barrier at a semiconductor-multiferroic interface. Patterned coatings of a metallic Ag with thickness $d \approx$ 400-500 nm and diameter of about 1 mm (evaporated thermally through a mask onto the top of BFO and BNFO films) as well as pads of metallic In attached mechanically to the conductive STON and Si substrates were used as electrodes for the electrical transport measurements.

3 Results and discussion XRD Θ-2Θ spectra of the synthesized BFO ceramics certified presence of a rhombohedral structure with space group R3c, lattice parameter a_{rh} = 0.396 nm and α = 89.45°. Slightly lower value of the lattice parameter a_{rh} and higher α value (0.395 nm and 89.45°) have been indicated from XRD spectra of the ceramic BNFO samples. This observation is in a good accordance to recent data [4]. Thus, one can conclude that Bi in the doped material is partially substituted by Nd ions and the rhombohedral distortion is slightly reduced with doping by Nd.

Similar XRD spectra measured for the undoped BFO/STO(100) films revealed growth of highly oriented perovskite-like BFO phase with certain small part of [110]-axis oriented crystallites and negligible amount of impurity phase ($Bi_{36}Fe_2O_{57}$). Meanwhile, XRD reflexes of the BNFO films showed single phase material with the off-plane lattice parameter of a pseudocubic unit cell of about 3.95 nm. Thus, we conclude that partial substitution of Bi^{3+} by Nd^{3+} with slightly reduced ionic radii (r_{Nd} = 1.08 Å and r_{Bi} = 1.20 Å) stabilizes formation of $BiFeO_3$ phase and reduces appearance of impurity phases such as $Bi_{36}Fe_2O_{57}$, $Bi_2Fe_4O_9$ and Fe_2O_3.

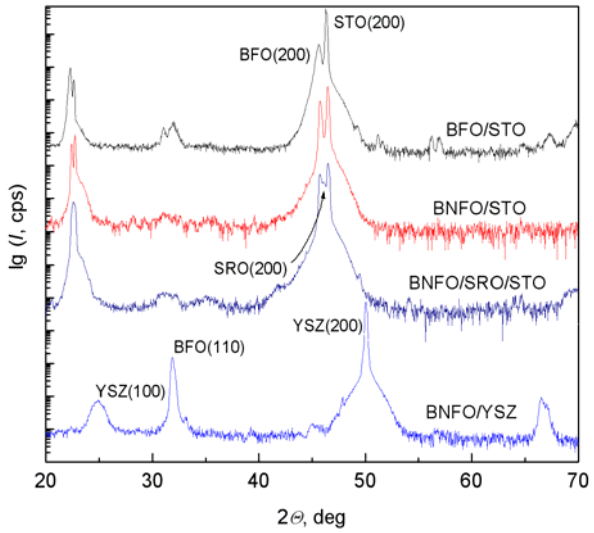

Figure 1 Θ-2Θ scans of $BiFeO_3$ and $Bi_{0.9}Nd_{0.1}FeO_3$ films grown by RF magnetron sputtering on crystalline $SrTiO_3$ (100), YSZ(100) substrates and metallic $SrRuO_3/SrTiO_3$(100) films.

All the films grown on lattice-matched STO(100), STON(100) and SRO(100) demonstrated cube-on cube growth mode. However, it is worth noting also growth of highly (110)-axis oriented BNFO film material on YSZ(100) substrate (see the corresponding XRD spectrum in Fig. 1). Finally, all the films grown on Si(111) with preliminary removed native oxide layer were polycrystalline with randomly oriented grains. Similar lattice parameter of a pseudocubic cell (a_c≅0.395 nm) has been indicated for the films grown on different substrates (STO, STON, YSZ).

AFM surface image of the BNFO films grown on the lattice-matched STO(100), STON(100) substrates and SRO(100) films demonstrated relatively smooth surface with average grain size of about 200 nm and surface roughness of about 15-30 nm.

The BFO and BNFO films grown on STO and YSZ substrates were semitransparent. Depending on their thickness they demonstrated yellow to brown color. The relative optical transmittance of two BNFO/YSZ films (d = 300 nm and 150 nm), $t = I_{fs}/I_s$ (here I_{fs} and I_s are intensities of light transmitted though a film and a substrate and that through a substrate), measured at room temperature (T = 293 K) in the wavelength range 300 to 3000 nm is shown in Fig. 2. The absorption coefficient, α, has been estimated both for doped (BNFO) and undoped (BFO) thin films.

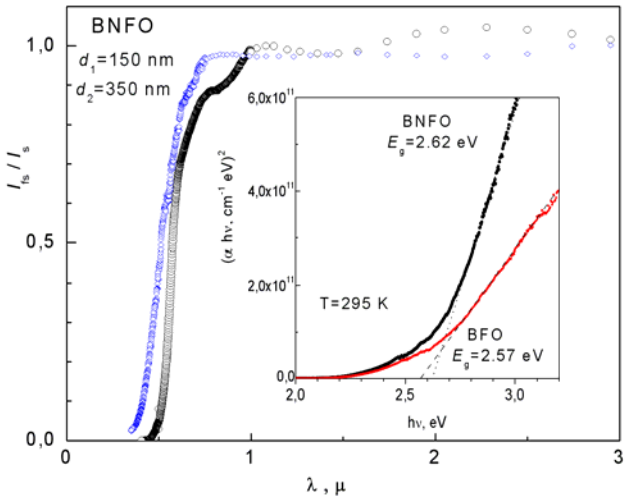

Figure 2 Optical transmittance of two BNFO /YSZ films and $(\alpha\ h\nu)^2$ versus photon energy plots of the BFO/YSZ and BNFO/YSZ films.

The plots of $(\alpha\ h\nu)^2$ versus photon energy ($h\nu$) of the BFO/YSZ and BNFO/YSZ films are displayed in Fig. 2. Clearly defined linear α^2 versus $h\nu$ regions seen from the figure at $h\nu > 2.6$ eV both for BFO and BNFO films demonstrate the well known absorption low $\alpha \sim (h\nu - E_g)^{1/2}$, being

characteristic for direct optical transitions between valence and conduction bands. The characteristic band gaps of the BFO and BNFO films of 2.57 eV and 2.62 eV (at T = 295 K), respectively, have been derived by extrapolating linear parts of the curves to the photon energy ($h\nu$) axis at $\alpha = 0$. The E_g value of BFO determined in this way is in a good agreement to recent data of other authors [8-10].

Following Fig. 2 we point out additional absorption for the BFO and BNFO films with the onset at approximately the same energy $E = E_a \cong 2.20$ eV. It is worth noting that similar absorption in the same energy range has been reported for $BiFeO_3$ films earlier [8]. The onset of optical absorption (at 2.17 eV) has been explained taking into account *d-d* excitations. The E_g and E_0 values derived for the BFO and BNFO films are summarized in Table 1.

Table 1 Band gap (E_g) and onset of absorption edge (E_a) of the grown multiferroic films derived from optical transmittance data.

Oxide film	Substrate	E_g, eV	E_a eV
$BiFeO_3$	YSZ(100)	2.57	2.20
$Bi_{0.9}Nd_{0.1}FeO_3$	YSZ(100)	2.62	2.20

Figure 3 shows linear-linear and log-linear (see inset in the same figure) plots of current-voltage (*I-U*) relations measured for the Ag/BFO/n-Si and Ag/BNFO/n-Si heterostructures at T = 300 K and 78 K. Complicated current-voltage (*I-U*) relations and clearly defined rectifying properties (in respect to current direction change) have been indicated for the device structures measured both at room temperature and at T = 78 K.

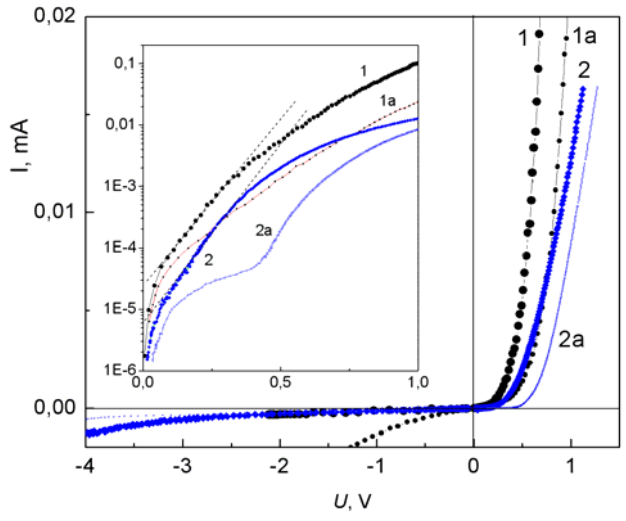

Figure 3 Current (I) versus voltage (U) relations of the Ag/$BiFeO_3$/n-Si (curves 1, 1a) and the Ag/$Bi_{0.9}Nd_{0.1}FeO_3$/n-Si (curves 2, 2a) heterostructures measured at 300 K (1, 2) and 78 K (1a, 2a). Semilog. plot of the same $I(U)$ dependencies in a case of a forward bias is shown in the inset

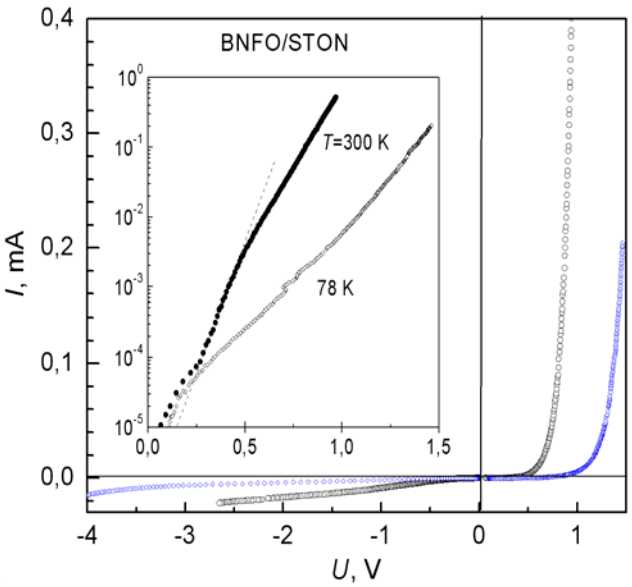

Figure 4 Current (I) versus voltage (U) relations of the Ag/n-$SrTiO_3$ < 0.7% Nb> heterostructures measured at 300 K and 78 K. Semilog. plot of the same $I(U)$ dependencies at a forward bias is shown in the inset

The *I-U* characteristics following the power low: $I \sim U^m$ with $m \cong 1.0$-1.1 have been indicated for the heterostructures at low bias voltage values ($|U| \leq 0.2$ V). The values of differential resistance at zero bias, $R_d(U = 0) = dU/dI$, of about 5.0 MΩ and 2.0 MΩ have been estimated for the Ag/BNFMO/Si and Ag/BFO/Si heterostructures at T = 300 K while significantly higher $R_d(U = 0)$ values have been found for the same heterostructures at T = 78 K.

It can be seen from Fig. 3 that the current flowing in a forward direction (positive voltage applied on the top Ag electrode) increased dramatically with U just after exceeding a certain critical value U_c (corresponding to the so called diffusion voltage introduced in the theory of a semiconductor p-n junction). A monotonic increase of U_c values and the corresponding shift of the step-like *I-U* branches to higher forward bias values have been indicated with temperature decreasing down to 78 K for both heterostructures.

Similar current-voltage (*I-U*) relations demonstrating rectifying properties have been measured for the Ag/BNFO/STON heterostructures at T = 300 K and 78 K (see Fig. 4). At room temperature, linear *I-U* relation has been measured for the heterostructure at low U values (<0.2 V) meanwhile a power low: $I \sim U^m$ (with $m \cong 1.5$-2.2) has been indicated at T = 78 K with U increasing up to about 0.5 V. The increase of differential resistance, $R_d(U = 0)$, from about 1.0 to 6.0 MΩ have been indicated for the heterostructure with cooling down to 78 K.

Clearly defined rectifying properties and linear portions of the *I-U* relations seen in Fig. 3 and Fig. 4 demonstrate dominating role of Shottky thermoelectronic emission at least at a certain intermediate range of forward bias

values. Meanwhile significant deviation from the linear *I-U* relations at higher *U* values could be explained assuming that at higher bias voltages current could be limited by series resistance related either to a bulk resistance of a multiferoic film (due to a Poole-Frenkel emission, hopping conduction and space charge-limited conduction [11]) or certain additional resistance of electrical contacts.

Current flowing through a uniform metal–semiconductor interface due to thermoelectronic emission in a case of forward bias can be expressed as [10]:

$$I = I_0\left[\exp\left(\frac{q(U - IR_s)}{nkT}\right) - 1\right]$$

here q is the electron charge, U is the forward bias voltage, n is the ideality factor demonstrating deviation of the experimental *I-U* data from the ideal thermoionic model, T is the absolute temperature, R_s is the series resistance and I_0 is the saturation current (derived from the straight line intercept of ln I at $U = 0$):

$$I_0 = AA^*T^2\exp\left(-\frac{q\Phi_{b0}}{kT}\right)$$

where A is the effective junction area, k is the Boltzmann constant, A^* is the effective Richardson constant (A* = 112 A $cm^{-2}K^{-2}$ assuming effective mass of carriers to be equal to that of free electron) and Φ_{b0} is the activation energy (the zero-bias barrier height).

Major electrical parameters, namely, the ideality factor (n), and the barrier height (Φ_{b0}) derived for the Ag/BFO; BNFO/Si and Ag/BNFO/STON heterostructures by fitting numerical *I-U* curves to the experimental points are summarized in Table 2. Following this table we mention similar values of the activation energy (0.82 eV and 0.84 eV) estimated for the BFO/Si and BNFMO/STON heterostructures at 300 K, respectively.

Table 2 Major electrical parameters: the ideality factor (n), and the barrier height (Φ_{b0}) derived for the Ag/BFO; BNFO/Si and Ag/BNFO/STON heterostructures from their *I-U* plots at 300 K.

Oxide film	n	Φ_{b0}, eV
BFO/n-Si	1.6	0.82
BNFO/n-Si	1,5	0,84
BNFO/STON	1.35	0,91

Relatively high values of series resistance estimated for the BFO/Si heterostructure are, probably, related to a possible formation of thin SiO_2 interlayer in the interface.

Complicated shape of the *I-U* curves of both the BFMMO/STON and (BFO, BNFO)/Si heterostructures measured at $T = 78$ K demonstrates, probably, presence of several electrical transport mechanisms. Following our results, we point out increasing role of space charge limited current [11] in the BFO films with temperature decreasing.

Summarizing, we conclude that high crystalline quality $BiFeO_3$ and $Bi_{0.9}Nd_{0.1}FeO_3$ (BNFO) films have been grown on various lattice matched substrates by RF sputtering. Optical transmittance spectra measured for the BFO and BNFO films certified presence of a direct bandgap with the characterictic energies E_g of 2.57 eV and 2.62 eV (at $T = 300$ K) for the undoped and doped materials, respectively, although an additional weak absorption with an unset at 2.20 eV has been indicated.

The current-voltage dependencies of the heterostructures prepared by growing the BFO and BNFO films on both Si and Nb-doped $SrTiO_3$(100) demonstrated clearly defined rectifying properties. Schottky junction model has been applied for the heterojunctions at $T = 300$ K although complicated shape of the *I-U* curves demonstrated increasing role of the space charge limited current with T decreasing down to 78 K.

Acknowledgements The work has been supported partially by Lithuanian government and National Science and Education of Lithuania (Grant C-18)

References

[1] Y. Hosono and M. Febig, J. Phys. D **38**, R123 (2005).
[2] J. Wang et al., Science **299**, 1719 (2003).
[3] G. A. Smolenskii and I. E. Chupis, Sov. Phys. Usp. 25, 475 (1982).
[4] G. L. Yuan, S. W. Ora, J. M. Liu, and G. Liu, Appl. Phys. Lett. **89**, 052905 (2006)
[5] B. Yu, M. Li, J. Liu, D. Guo, L. Pei, and X. Zhao. J. Appl. Phys. **41**, 06503 (2008).
[6] X.Qi, J. Dho, R. Thomov, M. G. Blamire, anf J. L. MacManus-Driscol, Appl. Phys. Lett. **86**, 062903 (2005).
[7] H. Yang, H. M. Luo, H. Wang, I. O. Usov, N. A. Suvorova, M. Jain, D. M. Feldmann, P. C. Dowden, R. F. DePaula, Q. X. Jia, G.-Z. Liu, C. Wang, C.-C. Wang, J. Qiu, M. He, J. Hing, K.-J. Jin, H. Bin, and G.- Z. Yang, Appl. Phys. Lett. **92**, 122903 (2008).
[8] S. R. Basu, W. Martin, Y. H. Chu, M. Gajek, R. Ramesh, R. Rai, X. Xu, and J. L. Musfeldt, Appl. Phys. Lett. **92**, 091905 (2008).
[9] V. Gopalan, S. W. Cheong, and J. L. Musfeldt, Phys. Rev. B 79, 134425 (2009); J. F. Ihlefeld, N. J. Podraza, Z. K. Liu, R. C. Rai, X. Xu, T. Heeg, Y. B. Chen, J. Li, R. W. Collins, J. L. Musfeldt, X. Q. Pan, J. Schubert, R. Ramesh, and D. G. Schlom, Appl. Phys. Lett. **92**, 142908 (2008).
[10] H. von Wenckstern, G. Biehne, R. A. Rahman, H. Hochmuth, M. Lorenz, and M. Grundmann, Appl. Phys. Lett. **88**, 092102 (2006).
[11] M. A. Lampert and P. Mark, Current Injection in Solids (Academic Press, New York, 1970).